Journal of Nuclear Science and Technology

ISSN: 0022-3131 (Print) 1881-1248 (Online) Journal homepage: https://www.tandfonline.com/loi/tnst20

Calculation of Gamma-Ray Buildup Factors up to Depths of 100 mfp by the Method of Invariant Embedding, (I)

Akinao SHIMIZU

To cite this article: Akinao SHIMIZU (2002) Calculation of Gamma-Ray Buildup Factors up to Depths of 100 mfp by the Method of Invariant Embedding, (I), Journal of Nuclear Science and Technology, 39:5, 477-486, DOI: 10.1080/18811248.2002.9715225

To link to this article: https://doi.org/10.1080/18811248.2002.9715225

Journal of NUCLEAR SCIENCE and TECHNOLOGY, Vol. 39, No. 5, p. 477–486 (May 2002)

Calculation of Gamma-Ray Buildup Factors up to Depths of 100 mfp by the Method of Invariant Embedding, (I)

Analysis of Accuracy and Comparison with Other Data

Akinao SHIMIZU*

The Wakasa Wan Energy Research Center, 64-52-1, Nagatani, Tsuruga-shi, Fukui 914-0192

(Received January 10, 2002 and accepted in revised form February 19, 2002)

The method of invariant embedding has been applied to calculations of gamma-ray buildup factors for point isotropic sources in infinite homogeneous media up to depths of 100 mean free paths (mfp) without bremsstrahlung. A comprehensive survey of buildup factors was performed to estimate errors due to energy, angle and space meshes adopted in the transport calculations by the present method. It is confirmed numerically that the exposure buildup factors can be calculated up to depths of 100 mfp with an error less than 10% by using the present method. The exposure buildup factors for water, iron and lead for typical source energies of 10 MeV, 1.0 MeV and 0.1 MeV are provided up to depths of 100 mfp. Those buildup factors are found to agree well with other data including the moments method calculations and the Monte Calro calculations by EGS4. These results indicate that the method of invariant embedding is able to provide gamma-ray buildup factor up to depths of 100 mfp with an accuracy enough to be used in shielding calculations.

KEYWORDS: buildup factor, radiation transport, radiation shielding, gamma radiation, point isotropic sources, invariant embedding method, multiple scattering, multi-group approximation, discrete ordinates approximation, radiation beam

I. Introduction

The gamma-ray buildup factors for point isotropic sources in infinite homogeneous media have been widely used in gamma-ray shielding calculations combined with the point kernel method. Considerable effort has been devoted to developing methods of calculating buildup factors taking into account multiple scattering of gamma-ray. The data set of gamma-ray buildup factors was first developed by Goldstein and Wilkins[1] based on the moments method. The comprehensive data set of buildup factors was further developed by the American Nuclear Society[2] in 1991. The relevant data were obtained based both on the moments method calculations for low-Z elements and on the calculations using the PALLAS code[3] for high-Z elements up to depths of 40 mean free paths (mfp). The geometrical progression formula derived by Harima[4] is also included in the ANS set as the fitting formula. The ANS data set has been currently used in shielding calculations as the standard. A detailed historical review on buildup factor calculation and use is given by Harima.[5]

After the publication of the ANS data, the exposure buildup factors for water, iron and lead for three typical energies of 10 MeV, 1.0 MeV and 0.1 MeV were obtained up to depths of 40 mfp by Hirayama[6] using the EGS4 Monte Carlo code with a particle splitting. The EGS4 data agree well with the ANS data except for iron at 10 MeV and for lead at 0.1 MeV and 10 MeV, where some discrepancies are found.

Kistos *et al.*[7] calculated the exposure buildup factors for some materials up to depths 30 mfp by using the SN1D code based on the discrete ordinates method. Their work aims at taking into account the effect of incoherent and coherent scatterings. Their computation scheme using the SN1D code[8] was further improved to include secondary sources of bremsstrahlung and fluorescence in the calculation of buildup factors.

The exposure buildup factors for water, iron and lead were also calculated up to depths of 40 mfp without bremsstrahlung by using the Angular Eigenvalue Method developed by the author[9] based on the method of invariant embedding.

Recently, the exposure buildup factors were calculated for several materials at 5 typical energies up to depths of 60 mfp by Chibani[10] using the Monte Carlo code EBUF. The relevant data include the effects of incoherent and coherent scatterings and secondary sources of bremsstrahlung and fluorescence.

The present work has been made to generate an advanced set of gamma-ray buildup factors for point isotropic sources in infinite homogeneous media based on the method of invariant embedding. The objectives of the work are as follows.

(1) Extension of the Buildup Factor up to Depths of 100 mfp

Some shielding calculations for a postulated severe accident of nuclear power reactor requires the gamma-ray buildup factors beyond depths of 40 mfp.

(2) Estimation of Error Associated with the Radiation Transport Method

Errors of the buildup factors due to the transport methods were neither provided quantitatively in the ANS set nor in the Monte Carlo calculations using a variance reduction technique. In the present work, errors associated with the transport calculations by the invariant embedding method shall be estimated quantitatively up to depths of 100 mfp.

(3) Inclusion of Bremsstrahlung

As pointed out by Hirayama,[6] the contribution of bremsstrahlung to the exposure buildup factors for iron and lead at 10 MeV in the ANS data set is overestimated. In the present work, an improvement on the treatment of

*Corresponding author, Tel. +81-770-24-2300, Fax. +81-770-24-5605, E-mail: ashimizu@werc.or.jp

bremsstrahlung shall be attempted.

(4) Consistent Use of the Cross Section Set

The buildup factors in the ANS data were computed with mixed sets of cross sections, NBS set[11] for low-Z elements and PHOTOX set[12] for high-Z elements. In the present work, the buildup factors of all elements shall be computed consistently with the specific set of cross sections.

Although it was reported by Hirayama and Trubey,[13] Kistos *et al.*[7] and Chibani[10] that effects of coherent and incoherent scattering on buildup factors at low energy are substantial, the buildup factors to be generated in the present work is based on the Compton scattering of gamma-ray with the free-electron. The buildup factor computed with coherent and incoherent scattering should be used combined with the mass attenuation coefficient including both coherent and incoherent scattering cross sections. In the present work, we shall generate a set of buildup factors in the traditional form to be used with the mass attenuation coefficient without coherent as defined by Hubbell[11] including free-electron Compton scattering cross section.

The purpose of this article is to present the results of the work aiming at the objectives (1) and (2). It includes an outline of the method of invariant embedding, an analysis of errors associated with transport calculations by the present method and the results of comparisons with exposure buildup factors obtained by other methods. The work including an improved treatment of bremsstrahlung and a generation of an advanced set of buildup factors is in progress, and will be presented in the article to be followed.

II. Method of Invariant Embedding

The method of invariant embedding was introduced by Ambarzumian[14] and further developed by Chandrasekhar[15] and Bellman and Kalaba.[16] It was further extended and applied to the gamma-ray transport problems with real energy and angle-dependent cross sections by the authors.[17–20] Recently, a set of gamma-ray albedos data for semi-infinite media was generated by Kadotani and the author.[21] A new method of solution for the invariant embedding equation called "Angular Eigenvalue Method" was developed by the author.[9]

In this chapter, an outline of the invariant embedding method is described. More detailed description is found elsewhere.[9,20]

1. Equation and Functional Relation

The modified transmission function $\tilde{T}(E,\ \omega|E_0,\ \omega_0;\ X)$ for a slab of thickness X is defined by the equation

$$J_t(E,\ \omega;\ X) = \int_0^{E_0} dE' \int_0^1 d\omega' \tilde{T}(E,\ \omega|E',\ \omega';\ X) \times J_s^+(E',\ \omega'), \tag{1}$$

where $J_s^+(E,\ \omega)$ represents the current density of gamma-ray with energy E in the forward direction ω from a source placed in front of a semi-infinite homogeneous medium and $J_t(E,\ \omega;\ X)$, the current density of gamma-ray transmitted through a homogeneous slab of thickness X placed in front of the plane source with the same composition as the semi-infinite medium. It can be proved physically that the modified transmission function satisfies the functional relation

$$\tilde{T}(E,\ \omega|E_0,\ \omega_0;\ X+X') = \int_0^{E_0} dE' \int_0^1 d\omega' \times \tilde{T}(E,\ \omega|E',\ \omega';\ X')\tilde{T}(E',\ \omega'|E_0,\ \omega_0;\ X). \tag{2}$$

The equation for the modified transmission function was first derived by the author.[18] Based on the multi-group approximation with respect to energy and the discrete ordinates approximation with respect to the angular variable, the desired equation is expressed as

$$\frac{d}{dX}\boldsymbol{y}^{(n)}(X) = \boldsymbol{A}^{(n)}\boldsymbol{y}^{(n)}(X) + \boldsymbol{b}^{(n)}(X) \qquad n = m,\ m+1,\ \cdots N. \tag{3}$$

Here, we divide the energy range of interest into N groups and the range of the angular variable $0 \leq \omega \leq 1$ into G sub-regions such as $\{\bar{\omega}_{k-1} \leq \omega \leq \bar{\omega}_k;\ k = 1,\ 2,\ \ldots\ G\}$, where $\bar{\omega}_{k-1}$ and $\bar{\omega}_k$ are the boundary values of the sub-region k and $\bar{\omega}_0 = 0$ and $\bar{\omega}_G = 1$. $\boldsymbol{y}^{(n)}(X)$ in Eq. (3) is the column vector of the dimension G, the element of which is given by

$$y_i^{(n)}(X) = \tilde{T}_{nm}(\omega_i,\ \omega_j;\ X) \quad i = 1-G. \tag{4}$$

$\tilde{T}_{nm}(\omega_i,\ \omega_j;\ X)$ represents the modified transmission function from the group m to n and from the angular division ω_j, the mid value of ω in the sub-region j, to ω_i defined by

$$\tilde{T}_{nm}(\omega_i,\ \omega_j;\ X) = \frac{1}{\Delta E_m}\int_n dE \int_m dE_0 \times \tilde{T}(E,\ \omega_i|E_0,\ \omega_j;\ X), \tag{5}$$

where $\int_n dE$ represents the integration over the group n and ΔE_m, the width of the group m respectively.

$\boldsymbol{A}^{(n)}$ is the matrix of the dimension G, the element of which is given by

$$a_{ij}^{(n)} = -\frac{\Sigma_n}{\omega_i}\delta_{ij} + w_j C_{nn}(\omega_i,\ j), \tag{6}$$

where

$$\Sigma_n = \frac{1}{\Delta E_n}\int_n dE\, \Sigma(E), \tag{7}$$

and

$$C_{nm}(\omega_i,\ j) = \frac{1}{\Delta E_m w_j}\int_n dE \int_m dE_0 \int_{\omega_j^-}^{\omega_j^+} d\omega \times C(E,\ \omega_i|E_0,\ \omega), \tag{8}$$

and w_j is the width of the angular sub-region j, and δ_{ij}, the Kronecker delta. $\Sigma(E)$ in Eq. (7) is the gamma-ray total macroscopic cross section of the medium. The function $C(E,\ \omega|E_0,\ \omega_0)$ in Eq. (8) is defined by

$$C(E,\ \omega|E_0,\ \omega_0) = \frac{1}{\omega_0}\Sigma_s(E_0,\ \omega_0 \to E,\ \omega) + \frac{1}{\omega_0}\int_0^{E_0} dE' \int_0^1 d\omega' \times R(E,\ \omega|E',\ \omega';\ \infty) \times \Sigma_s(E_0,\ \omega_0 \to E',\ -\omega'), \tag{9}$$

where $\Sigma_s(E_0,\ \omega_0 \rightarrow E,\ \omega)$ is the macroscopic double differential cross section for scattering from energy E_0 to E and from the direction ω_0 to ω, and $R(E,\ \omega|E_0,\ \omega_0;\ \infty)$ represents the reflection function for the semi-infinite medium behind the source.

$\boldsymbol{b}^{(n)}(X)$ is the column vector of the dimension G, the element of which is given by

$$b_i^{(n)}(X) = \sum_{l=m}^{n-1}\sum_{k=1}^{G} w_k C_{nl}(\omega_i,\ k)\tilde{T}_{lm}(\omega_k,\ \omega_j;\ X), \quad (10)$$

Eq. (3) should be solved subject to the initial condition

$$\tilde{T}_{nm}(\omega_i,\ \omega_j;\ 0) = \frac{1}{w_i}\delta_{nm}\delta_{ij}. \quad (11)$$

2. Method of Solution

Two kinds of method were developed by the author to solve Eq. (3) subject to the initial condition (11):

(1) the angular eigenvalue method[9)]

(2) the method of direct numerical integration.[18,20)]

According to the angular eigenvalue method, Eq. (3) is solved analytically with respect to the slab thickness X. The solutions are expressed in terms of a linear combination of the exponential functions $\{\exp(\lambda_{ni}X) :\ n{=}m-N,\ i{=}1-G\}$, where the constants $\{\lambda_{ni};\ i{=}1-G\}$, called the angular eigenvalue, are determined as the eigenvalues of the matrix $\boldsymbol{A}^{(n)}$.

According to the direct numerical integration method, Eq. (3) is integrated numerically with respect to the slab thickness X by using the Runge-Kutta method for the first step. The solutions for extended thickness are obtained by using the functional relation equivalent with Eq. (2):

$$\tilde{T}_{nm}(\omega_i,\ \omega_j;\ X+X') = \sum_{l=m}^{n}\sum_{k=1}^{G} w_k \tilde{T}_{nl}(\omega_i,\ \omega_k;\ X') \times \tilde{T}_{lm}(\omega_k,\ \omega_j;\ X). \quad (12)$$

3. Buildup Factor for Point Isotropic Source

We define the energy-dependent number buildup factor for a point isotropic source in an infinite homogeneous medium $B^{pt}(E,\ X)$ by the equation

$$\phi^{pt}(E,\ X) = B^{pt}(E,\ X)\exp(-\Sigma(E_0)X)/(4\pi X^2), \quad (13)$$

where $\phi^{pt}(E,\ X)$ represents the flux density of gamma-ray with energy E at the distance of X from the point isotropic source with energy E_0. The corresponding energy dependent exposure buildup factor can be obtained by multiplying $B^{pt}(E,\ X)$ with the factor $(E\Sigma_{en,\mathrm{air}}(E)/E_0\Sigma_{en,\mathrm{air}}(E_0))$, where $\Sigma_{en,\mathrm{air}}(E)$ represents the energy absorption cross section of air. Based on the fact that the plane source is an assemble of the point isotropic sources distributed uniformly on the plane, we get the equation

$$B^{pt}(E,\ X) = -2X\exp(\Sigma(E_0)X)\frac{d}{dX}\phi^{pl}(E,\ X), \quad (14)$$

where $\phi^{pl}(E,\ X)$ represents the flux density due to the corresponding plane isotropic source in the infinite medium. The flux $\phi^{pl}(E,\ X)$ can be obtained from the modified transmission function and the reflection function for the semi-infinite medium. Equation (14) includes the derivative of $\phi^{pl}(E,\ X)$ with respect to X, that can be performed analytically for the solution obtained by the angular eigenvalue method. The desired derivative for the solution obtained by the direct numerical integration method can be computed by using Eq. (3) where it is given by the right hand side of the equation. The application of the direct numerical integration method to calculations of point isotropic buildup factors is new, and first presented in this paper.

III. Analysis of Error

The source of error in the calculation of buildup factors includes cross section uncertainties and errors associated with the transport method used. In the present chapter, errors associated with the transport calculations by the method of invariant embedding are estimated quantitatively up to depths of 100 mfp.

1. Survey Calculation for Error Analysis

A comprehensive survey for exposure buildup factors was performed to estimate errors due to energy, angle and space meshes adopted in the present method.

The scope of the survey is as follows (**Table 1**):

Material: Water, iron and lead.

Energy region: Five energy regions A, B, C, D and E are specified corresponding to the source energies of 10 MeV, 1.0 MeV, 0.2 MeV, 0.1 MeV and 0.08 MeV respectively. The upper boundary energy of the region is determined so that the average energy of the first group in the multi-group approximation is equal to the specified source energy. The lower boundary energy is chosen so that the ratio of exposure buildup factor integrated in the specified energy region to that integrated over the whole energy is greater than 0.85. The selected energy range does not include the K edge for lead, since the K edge should be treated with a particularly fine energy mesh.

Energy group: Total number of energy groups for the specified energy region is varied from 5 to 80 with equal mesh width to check the influence of the energy mesh upon buildup factors.

Angular division: Gaussian quadrature set in the range $0{\leq}\omega{\leq}1$ is used. The number of angular divisions is varied from 5 to 15 to check the influence of the angular mesh upon buildup factors.

Secondary source: Only the Compton scattering with free-electron is included.

The exposure buildup factors for about 500 cases covering the combinations of materials, energy regions (source energies), number of energy groups and number of angular divisions were computed up to depths of 100 mfp.

2. Influence of the Space Mesh

The influence of the space mesh upon exposure buildup factors is checked by comparing the solution obtained by the direct numerical integration method (NI method) with that obtained by the angular eigenvalue method (AE method). Although the latter solution is given analytically with respect to the depth, it may have a rounding off error when an angular

Table 1 Scope of survey for error analysis of exposure buildup factors

Energy region	Source energy	Material	Energy range (MeV)	Number of energy groups	Number of angular divisions
A	10.0 MeV	Water	$10.0+\alpha^{a)}-1.0^{b)}$	10 – 80 Equal mesh width	5 – 15 Gaussian quadrature in the range $0\leq\omega\leq1$
		Iron	$10.0+\alpha-1.0$		
		Lead	$10.0+\alpha-1.0$		
B	1.0 MeV	Water	$1.0+\alpha-0.05$		
		Iron	$1.0+\alpha-0.2$		
		Lead	$1.0+\alpha-0.2$		
C	0.2 MeV	Water	$0.2+\alpha-0.035$		
		Iron	$0.2+\alpha-0.10$		
		Lead	$0.2+\alpha-0.15$		
D	0.1 MeV	Water	$0.1+\alpha-0.030$		
		Iron	$0.1+\alpha-0.088$		
		Lead	$0.1+\alpha-0.088$		
E	0.08 MeV	Water	$0.08+\alpha-0.025$		
		Iron	$0.08+\alpha-0.06$		
		Lead	$0.08+\alpha-0.06$		

a) α is determined so that the average energy of the first group is equal to the source energy.
b) Lower boundary energy is chosen so that ratio of buildup factor integrated in the energy region to that integrated in the whole energy is greater than 0.85.

Table 2 Influence of space mesh upon exposure buildup factor calculation

Water, energy region B (source energy 1.0 MeV)

	BF(numerical)[a)]/BF(analytical)[b)]				
Depth/Δ	1/32 mfp	1/64 mfp	1/128 mfp	1/256 mfp	1/512 mfp
1.0 mfp	1.0944	1.0105	1.0011	1.0003	1.0003
10.0	1.1920	1.0223	1.0018	1.0001	1.0000
40.0	1.2057	1.0241	1.0019	1.0002	1.0001
70.0	1.2074	1.0243	1.0019	1.0001	1.0000
100.0	1.2081	1.0243	1.0019	1.0001	1.0000

a) Buildup factor obtained by the direct numerical integration method using Runge-Kutta method with initial mesh width Δ.
b) Buildup factor obtained analytically by the angular eigenvalue method.

eigenvalue happens to be very close to other one, since it is assumed in deriving analytical solutions that the angular eigenvalues differ with each other. **Table 2** presents comparisons of exposure buildup factors for water in the energy region B up to depth of 100 mfp. The difference between solutions by both methods decreases rapidly with the mesh width used in the integration by Runge-Kutta method for the first step in NI method. The difference is 0.03% or less up to depth of 100 mfp, when the mesh width of 1/512 mfp is used. The same results are obtained for other materials and other energy regions. The error due to space mesh in the present method is confirmed to be 0.03% or less up to depth 100 mfp, when the initial mesh width of 1/512 mfp or 1/1,024 mfp is used.

It should be mentioned here that the solutions for extended depths are efficiently obtainable by using the functional relation (12) starting from the solution for the depth as small as 1/1,024 mfp. Therefore, the present method is powerful to be applied to the deep penetration problems. Most calculations in the survey of exposure buildup factors were performed by using NI method, since NI method is faster than AE method. AE method was used to check the error due to the space mesh for some selected cases.

3. Influence of the Angular Mesh

We shall denote an exposure buildup factor computed with a number of angular divisions G and a number of energy groups N at a depth of X by $B(G,\ N;\ X)$.

(1) Correlation between Energy Mesh and Angular Mesh

Based on the survey, it is found that the influence of the angular mesh upon buildup factor does not correlate with the energy mesh under an appropriate condition. **Table 3** shows the exposure buildup factor ratios $\{B(G,\ N;\ X)/B(13,\ N;\ X);\ G=7-11\}$ calculated with number of energy groups $N=30,\ 40,\ 50$ for water in the energy region B. It indicates that the change of the ratios $\{B(G,\ N;\ X)/B(13,\ N;\ X);\ G=7-11\}$ with N is less than 0.2%, when $N\geq40$. The similar results are obtained for other materials and other energy regions. It is confirmed numerically that the buildup factor ratio $B(G',\ N;\ X)/B(G,\ N;\ X)$ is independent of the number of energy groups N, when G', $G\geq7$ and $N\geq20$ for the energy region A, $N\geq40$ for the energy regions B and C, $N\geq30$ for the energy regions D and E.

(2) Influence of the Angular Mesh

The exposure buildup factor ratios $\{B(G,\ N;\ X)/B(15,\ N;\ X);\ G=5-13\}$ are computed for all materials and energy regions. The relevant ratio is smaller than unity, and approaches unity when the number of angular divisions G increases.

(3) Limiting Error for Angular Mesh

The quantitative estimation of error requires not only buildup factor ratios $\{B(G,\ N;\ X)/B(15,\ N;\ X);\ G=5-13\}$ but also the error in the buildup factor $B(15,\ N;\ X)$ itself, that is unknown. Here, we have developed a method to pro-

Table 3 Ratio of exposure buildup factor calculated with different number of angular divisions and energy groups

Water, energy region B (source energy 1.0 MeV)

	7D/13D[a)]			9D/13D			11D/13D		
Depth/N[b)]	30	40	50	30	40	50	30	40	50
1 mfp	1.000	0.999	1.000	1.000	1.000	1.000	1.000	1.000	1.000
10	0.992	0.992	0.992	0.996	0.996	0.996	0.999	0.999	0.999
40	0.940	0.940	0.940	0.973	0.973	0.973	0.990	0.990	0.990
70	0.843	0.841	0.841	0.945	0.946	0.946	0.981	0.980	0.981
100	0.684	0.677	0.676	0.895	0.896	0.896	0.968	0.968	0.969

a) Ratio of buildup factor calculated with 7 angular divisions to that calculated with 13 angular divisions.
b) Number of energy groups.

vide a limiting value of the error in $B(15,\ N;\ X)$ under an appropriate condition.

We introduce an angular error coefficient defined by

$$Ea(G,\ X) = B(G,\ N;\ X)/B(\infty,\ N;\ X), \tag{15}$$

where $B(\infty,\ N;\ X)$ represents the exact value of exposure buildup factor to be obtained if G could be extended to infinite. The angular error coefficient is independent of the number of energy groups N under the condition described in the previous section. We further introduce a function $f(w_G,\ X)$ defined by

$$Ea(G,\ X) = \exp(f(w_G,\ X)), \tag{16}$$

where w_G represents the width of the angular mesh corresponding with the number of angular divisions G. It follows that $w_1>w_2>w_G>w_{G+1}>0$, $w_\infty=0$ and $f(0,\ X)=0$. The buildup factor ratio and the error coefficient can be rewritten as

$$B(H,\ N;\ X)/B(G,\ N;\ X) = \exp(f(w_H,\ X) - f(w_G,\ X)) = \exp\left(\int_{w_G}^{w_H} dw df/dw\right), \tag{17}$$

$$Ea(G,\ X) = \exp(f(w_G,\ X)) = \exp\left(\int_{0}^{w_G} dw df/dw\right). \tag{18}$$

The above equations indicate that both the buildup factor ratio and the error coefficient are given in terms of the area under the curve of the function df/dw.

When the function df/dw satisfies the condition of monotonic function: ⌈$|df/dw|$ decreases monotonically with w decreasing⌋, then it holds

$$|(\Delta f/\Delta w)_{w_G}|w_G > |(df/dw)_{w_G}|w_G > \left|\int_0^{w_G} dw df/dw\right|, \tag{19}$$

where

$$(\Delta f/\Delta w)_{w_G} = (f(w_H,\ X) - f(w_G,\ X))/(w_H - w_G) \qquad w_H > w_G. \tag{20}$$

The relative values in Eq. (19) are illustrated schematically in **Fig. 1**, where the area under the curve BC stands for the integral $|\int_0^{w_G} dw df/dw|$, the area under the line BD, the value $|(df/dw)_{w_G}|w_G$ and the area under the line EF, the value $|(\Delta f/\Delta w)_{w_G}|w_G$ respectively. Now, we introduce a limiting angular error coefficient defined by

$$\bar{E}a(G,\ X) = \exp(w_G(\Delta f/\Delta w)_{w_G}). \tag{21}$$

Since the angular error coefficient is less than unity and both the functions f and df/dw are negative, we get

$$\bar{E}a(G,\ X) < Ea(G,\ X). \tag{22}$$

The limiting angular error coefficients are actually computed based on the exposure buildup factors $\{B(G,\ N;\ X);\ G=5,\ 7,\ 9,\ 11,\ 13,\ 15\}$. The width of the sub-region G, that is closest to 1.0, in the Gaussian quadrature is chosen as the parameter w_G. The values of the function $(\Delta f/\Delta w)_{w_G}$ are computed by the equation

$$(\Delta f/\Delta w)_{w_G} = (f(w_{G-2},\ X) - f(w_G,\ X))/(w_{G-2} - w_G) \qquad G = 7,\ 9,\ 11,\ 13,\ 15, \tag{23}$$

and used to confirm the condition of the monotonic function. **Figure 2** shows the limiting angular error coefficients for water in the energy region B computed with the above procedure. The limiting angular error coefficients for $G=13$ for all materials and energy regions are given in **Table 4**. The condition of the monotonic function for the function $(\Delta f/\Delta w)_{w_G}$

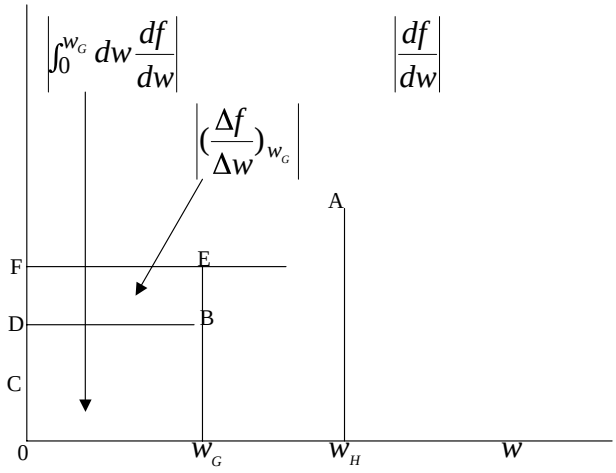

Fig. 1 Curve of the function df/dw and associated integrals

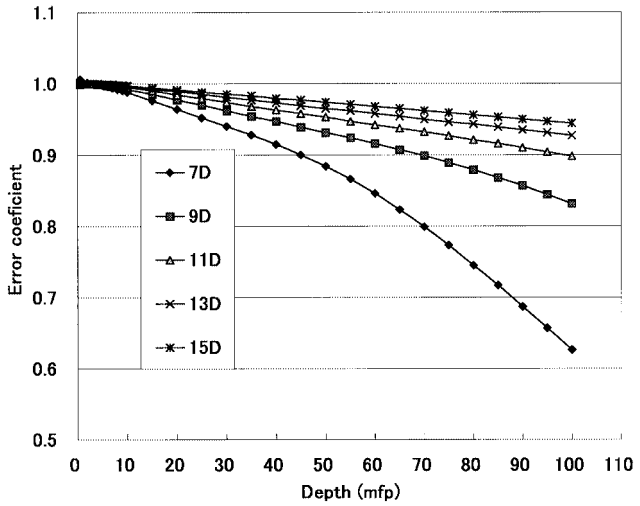

Fig. 2 Limiting angular error coefficient of exposure buildup factor for water in energy region B (source energy 1.0 MeV)
7D stands for the coefficient of buildup factor calculated with 7 angular divisions.

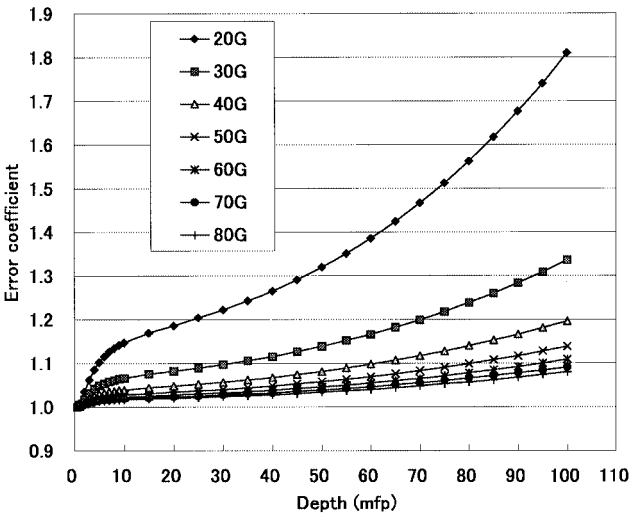

Fig. 3 Limiting energy error coefficient of exposure buildup factor for water in energy region B (source energy 1.0 MeV)
20G stands for the coefficient of exposure buildup factor calculated with 20 energy groups.

is confirmed to hold except for the case of water in the energy region A, where a slight oscillation is found. Since such oscillation of the function $(\Delta f/\Delta w)_{w_G}$ occur at the point where $(\Delta f/\Delta w)_{w_G}$ is close to zero and the corresponding limiting error coefficient is close to unity, it can be neglected for the practical estimation of error. It is confirmed numerically that the error due to the angular mesh associated with the transport calculation with 13 angular divisions is less than 10% up to depths of 100 mfp.

Kistos *et al.*[7] reported that an extremely fine angular mesh was required in their calculations of exposure buildup factors by the SN1D code. The error due to angular mesh was estimated 2% at depth of 30 mfp, when S_{64} Gaussian quadrature was applied. Our calculation with 13 angular divisions in the range $0 \leq \omega \leq 1.0$ corresponds to S_{26} discrete ordinates calculation. A reason for attaining a high accuracy with relatively rough angular mesh in our calculations is presumed as follows.

The double differential scattering cross sections from a group to the same group (within-group scattering) $\Sigma_{nn}(\omega, \omega_0)$ has a very strong anisotropy due to the energy-angle correlation in the scattering. For example, the scattering angle θ_s corresponding with within-group scattering in a energy group specified as $9.5\,\text{MeV} \leq E \leq 10.5\,\text{MeV}$ is limited by $1-0.00512 \leq \cos\theta_s \leq 1$, since the change in the Compton wave length corresponding with the within-group scattering is 0.00512 or less. The expansion of the double differential cross section $\Sigma_{nn}(\omega, \omega_0)$ in terms of the Legendre function $P_l(\omega)P_l(\omega_0)$, supposed to be used by Kistos *et al.*, converges very slowly and requires many terms, since the double differential cross section behaves almost like the delta function $\delta(\omega-\omega_0)$. In our procedure, the double differential cross sections are calculated analytically from Klein-Nishina formula taking into account the energy-angle correlation. Our procedure avoids the problem of slow convergence described above and makes us to attain a high accuracy with relatively rough angular mesh.

Table 4 Limiting angular error coefficient of exposure buildup factor calculated with 13 angular divisions

Material	Energy region /Depth	1.0 mfp	10 mfp	40 mfp	70 mfp	100 mfp
Water	A	1.000	0.997	0.996	1.009	0.968
	B	1.000	0.996	0.973	0.950	0.927
	C	1.000	0.999	0.985	0.970	0.954
	D	1.000	0.999	0.988	0.976	0.963
	E	1.000	0.999	0.989	0.977	0.965
Iron	A	1.000	0.997	0.967	0.938	0.914
	B	1.001	0.996	0.973	0.950	0.927
	C	1.000	0.998	0.984	0.971	0.954
	D	1.001	0.999	0.994	0.989	0.975
	E	1.000	0.999	0.996	0.993	0.980
Lead	A	1.000	0.998	0.973	0.946	0.917
	B	1.000	0.997	0.983	0.971	0.957
	C	1.000	1.000	0.998	0.996	0.979
	D	1.000	1.000	1.000	0.999	0.981
	E	1.000	1.000	0.999	0.998	0.981

4. Influence of the Energy Mesh

The same method of error analysis as described in the previous section is applied to estimate errors due to energy mesh.

(1) Correlation between Energy Mesh and Angular Mesh

Based on the survey, it is confirmed numerically that the exposure buildup factor ratio $B(G, N'; X)/B(G, N; X)$ between different numbers of energy groups is independent of the number of angular divisions G, when $G \geq 9$ and $N, N' \geq 15$ for the energy region A, $N, N' \geq 20$ for the energy regions B, C and D, and $N, N' \geq 30$ for the energy region E.

(2) Influence of the Energy Mesh

The exposure buildup factor ratios $\{B(G, N'; X)/B(G, N; X)\}$ are computed for all materials and energy re-

Table 5 Limiting energy error coefficient of exposure buildup factor

Material	Energy region	Number of energy groups/Depth	1.0 mfp	10 mfp	40 mfp	70 mfp	100 mfp
Water	A	30	1.001	1.003	1.014	1.042	1.088
	B	70	1.002	1.019	1.032	1.055	1.091
	C	60	1.000	1.003	1.022	1.052	1.097
	D	60	1.000	1.000	1.017	1.048	1.094
	E	70	1.000	1.000	1.016	1.048	1.095
Iron	A	15	1.001	1.015	1.035	1.053	1.073
	B	50	1.000	1.002	1.014	1.039	1.078
	C	60	1.000	1.001	1.014	1.043	1.087
	D	20	1.000	1.001	1.008	1.024	1.048
	E	30	1.000	1.001	1.014	1.042	1.084
Lead	A	40	1.000	1.003	1.022	1.042	1.064
	B	60	1.000	1.001	1.015	1.046	1.096
	C	15	1.000	1.001	1.011	1.033	1.062
	D	10	1.000	1.000	1.002	1.005	1.010
	E	10	1.000	1.001	1.021	1.051	1.079

Table 6 Gamma-ray exposure buildup factors for point isotropic sources

(Buildup factors at 10 MeV are calculated without bremsstrahlung.)

Material	Water			Iron			Lead		
Cross section	NBS29 (Ref. 11))			NBS29 (Ref. 11))			PHOTX (Ref. 12))		
Energy	10.0 MeV	1.0 MeV	0.1 MeV	10.0 MeV	1.0 MeV	0.1 MeV	10.0 MeV	1.0 MeV	0.1 MeV
R (mfp)									
0.5	1.21E+00	1.47E+00	2.39E+00	1.19E+00	1.41E+00	1.24E+00	1.13E+00	1.20E+00	1.60E+00
1.0	1.39E+00	2.08E+00	4.59E+00	1.34E+00	1.85E+00	1.39E+00	1.19E+00	1.37E+00	2.15E+00
2.0	1.70E+00	3.62E+00	1.19E+01	1.61E+00	2.85E+00	1.61E+00	1.33E+00	1.67E+00	3.48E+00
3.0	1.99E+00	5.53E+00	2.39E+01	1.89E+00	4.01E+00	1.78E+00	1.50E+00	1.95E+00	5.49E+00
4.0	2.28E+00	7.72E+00	4.15E+01	2.20E+00	5.31E+00	1.94E+00	1.71E+00	2.20E+00	8.80E+00
5.0	2.56E+00	1.02E+01	6.58E+01	2.54E+00	6.76E+00	2.07E+00	1.98E+00	2.44E+00	1.45E+01
6.0	2.84E+00	1.29E+01	9.78E+01	2.91E+00	8.33E+00	2.19E+00	2.31E+00	2.68E+00	2.45E+01
7.0	3.11E+00	1.59E+01	1.39E+02	3.32E+00	1.00E+01	2.31E+00	2.73E+00	2.90E+00	4.22E+01
8.0	3.38E+00	1.91E+01	1.89E+02	3.77E+00	1.18E+01	2.41E+00	3.26E+00	3.11E+00	7.40E+01
9.0	3.65E+00	2.26E+01	2.52E+02	4.25E+00	1.38E+01	2.51E+00	3.93E+00	3.32E+00	1.32E+02
10.0	3.91E+00	2.63E+01	3.27E+02	4.76E+00	1.58E+01	2.60E+00	4.77E+00	3.52E+00	2.37E+02
15.0	5.18E+00	4.79E+01	9.61E+02	7.94E+00	2.73E+01	3.00E+00	1.36E+01	4.44E+00	5.07E+03
20.0	6.41E+00	7.40E+01	2.23E+03	1.22E+01	4.09E+01	3.32E+00	4.09E+01	5.27E+00	1.24E+05
25.0	7.60E+00	1.04E+02	4.51E+03	1.79E+01	5.62E+01	3.59E+00	1.24E+02	6.04E+00	3.26E+06
30.0	8.75E+00	1.38E+02	8.30E+03	2.50E+01	7.31E+01	3.84E+00	3.72E+02	6.75E+00	8.96E+07
35.0	9.88E+00	1.74E+02	1.42E+04	3.39E+01	9.13E+01	4.05E+00	1.10E+03	7.43E+00	2.52E+09
40.0	1.10E+01	2.14E+02	2.32E+04	4.47E+01	1.11E+02	4.25E+00	3.18E+03	8.08E+00	7.16E+10
45.0	1.21E+01	2.56E+02	3.61E+04	5.78E+01	1.32E+02	4.43E+00	9.09E+03	8.69E+00	2.05E+12
50.0	1.32E+01	3.01E+02	5.42E+04	7.34E+01	1.53E+02	4.60E+00	2.56E+04	9.29E+00	5.91E+13
55.0	1.43E+01	3.49E+02	7.90E+04	9.17E+01	1.76E+02	4.76E+00	7.13E+04	9.87E+00	1.71E+15
60.0	1.53E+01	3.99E+02	1.12E+05	1.13E+02	2.00E+02	4.91E+00	1.96E+05	1.04E+01	4.96E+16
65.0	1.64E+01	4.51E+02	1.56E+05	1.38E+02	2.25E+02	5.05E+00	5.35E+05	1.10E+01	1.45E+18
70.0	1.75E+01	5.06E+02	2.12E+05	1.66E+02	2.50E+02	5.19E+00	1.45E+06	1.15E+01	4.23E+19
75.0	1.85E+01	5.62E+02	2.84E+05	1.99E+02	2.77E+02	5.32E+00	3.88E+06	1.21E+01	1.24E+21
80.0	1.96E+01	6.21E+02	3.74E+05	2.36E+02	3.04E+02	5.45E+00	1.03E+07	1.26E+01	3.65E+22
85.0	2.07E+01	6.82E+02	4.86E+05	2.78E+02	3.33E+02	5.56E+00	2.73E+07	1.31E+01	1.08E+24
90.0	2.17E+01	7.45E+02	6.23E+05	3.25E+02	3.62E+02	5.68E+00	7.19E+07	1.36E+01	3.19E+25
95.0	2.28E+01	8.10E+02	7.91E+05	3.79E+02	3.92E+02	5.79E+00	1.88E+08	1.41E+01	9.48E+26
100.0	2.39E+01	8.78E+02	9.94E+05	4.38E+02	4.22E+02	5.90E+00	4.90E+08	1.46E+01	2.82E+28

1.21E+00: Read as 1.21×10^{0}.

gions. The relevant buildup factor ratio is usually larger than unity, and approaches unity when the number of energy groups N increases.

(3) Limiting Error for Energy Mesh

We introduce the energy error coefficient and limiting energy error coefficient defined by the equations

$$Ee(N,\ X) = B(G,\ N;\ X)/B(G,\ \infty;\ X) = \exp(\ f(w_N,\ X)), \tag{24}$$

$$\bar{E}e(N,\ X) = \exp(w_N(\Delta f/\Delta w)_{w_N}), \tag{25}$$

where w_N represents the width of the energy mesh corresponding to the number of energy groups N. Since the energy error coefficient is usually greater than unity and both the functions f and df/dw are positive, we get

$$\bar{E}e(N,\ X) > Ee(N,\ X), \tag{26}$$

provided that the function df/dw satisfies the condition of monotonic function.

Figure 3 shows the limiting energy error coefficient for water in the energy region B. The limiting energy error coefficients for other materials and the energy regions are shown in **Table 5**. The condition for monotonic function for the function $(\Delta f/\Delta w)_{w_N}$ is confirmed to hold for all materials and the energy regions. It is confirmed numerically that the error in the exposure buildup factors integrated in the specified energy region due to the energy mesh is less than 10% up to depths of 100 mfp, when they are computed with the number of energy groups given in Table 5. Some additional energy groups, usually less than 10 groups, are required to compute the exposure buildup factor integrated over whole energy.

IV. Comparison with Other Calculations

The exposure buildup factors for water, iron and lead at typical source energies of 10 MeV, 1.0 MeV and 0.1 MeV are calculated up to depths of 100 mfp by the present method, and compared with other data including the buildup factors in the ANS data,[2] those obtained by Hirayama[6] by EGS4 Monte Carlo calculations (EGS4 data) and those obtained by Morris[22] by the moments method (Morris data). In order to eliminate the discrepancy due to the cross section set, the present calculations are performed with the same cross section set as that used in the calculations to be compared. The exposure buildup factors for water and iron are computed with NBS set,[11] and lead, with PHOTOX set.[12] The calculations include the annihilation of positrons and the fluorescence (KX-ray) as the secondary sources, but do not include the bremsstrahlung. The calculations are performed with from 13 to 15 angular divisions and from 60 to 80 energy groups. A limiting error computed by the procedure described previously is less than 5% at depths of 40 mfp and less than 10% at depths of 100 mfp.

Table 6 gives the exposure buildup factors obtained up to depths of 100 mfp. The ratio of the buildup factor obtained by the present method to that by other method is plotted as a function of depth in **Figs. 4**, **5** and **6**.

(1) Comparison with Moments Method Calculations

The exposure buildup factors for water and iron obtained by the present method (IE data) agree very well with ANS data obtained by using the moments method and Morris data. The discrepancy between both data is less than about 5% up to depth of 40 mfp, provided that Morris data is taken for comparison for water at the source energy of 0.1 MeV. The result of comparisons is consistent with the estimated limiting error at depths of 40 mfp in our calculations.

(2) Comparison with EGS4 Data

IE data agrees well with EGS4 data for all materials for all source energies. Discrepancy between both data is about 10% or less up to depths of 40 mfp. The result of comparison is consistent with the estimated limiting error at depth of

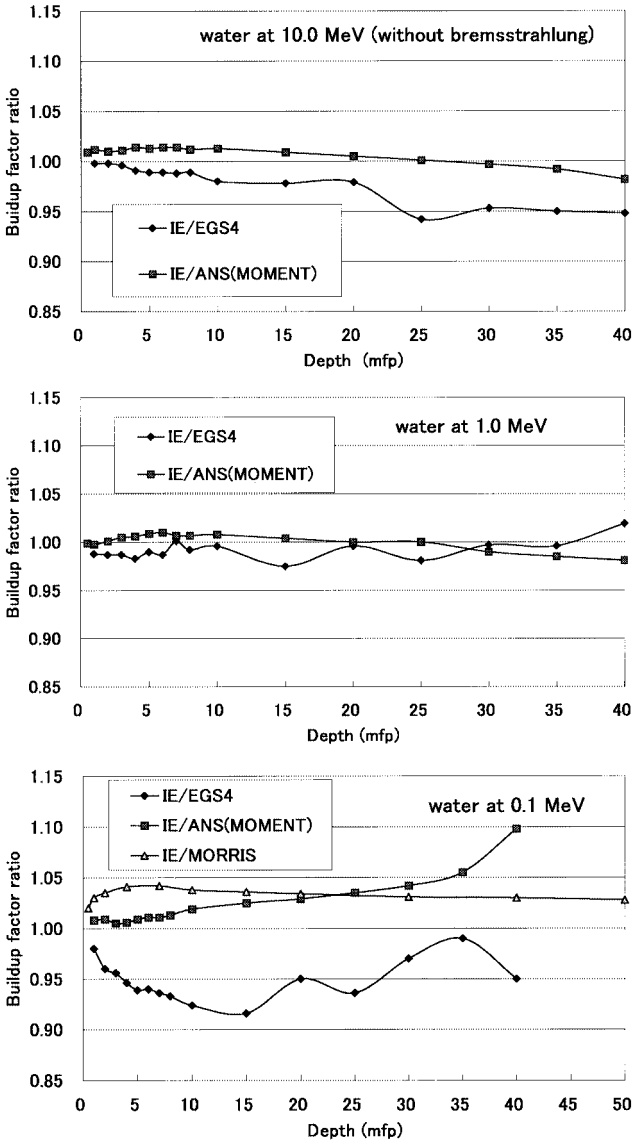

Fig. 4 Ratio of exposure buildup factor for water obtained by IE method to that obtained by other method
IE: Present calculation
EGS4: Buildup factor obtained by using EGS4[6]
ANS(MOMENT): Buildup factor in ANS standard obtained by the moments method[2]
MORRIS: Buildup factor obtained by Morris by the moments method[22]

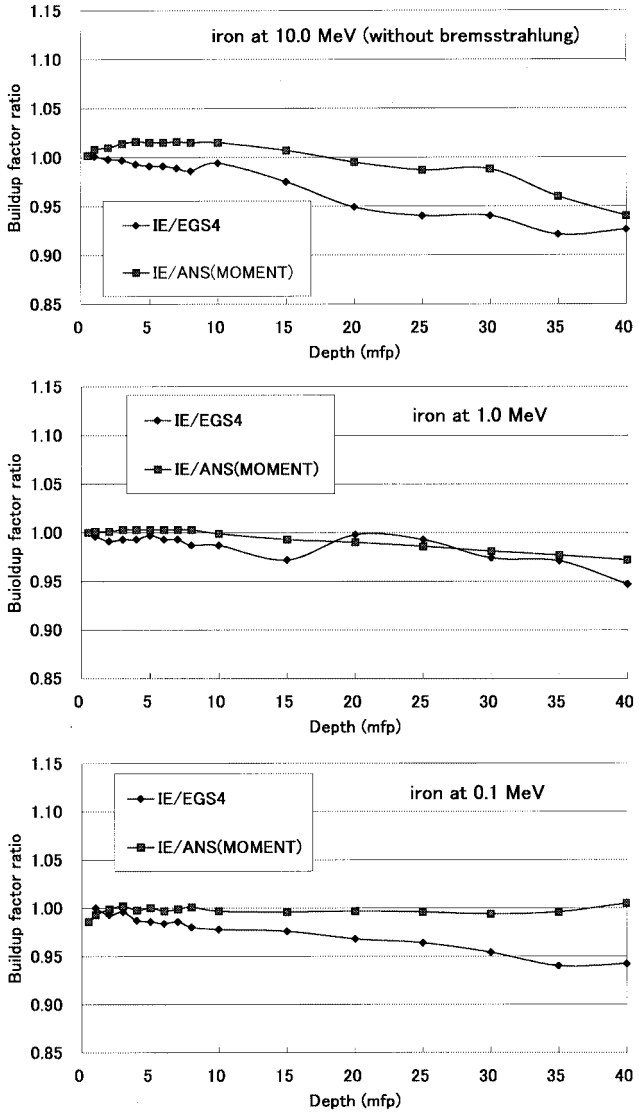

Fig. 5 Ratio of exposure buildup factor for iron obtained by IE method to that obtained by other method
IE: Present calculation
EGS4: Buildup factor obtained by using EGS4[6)]
ANS(MOMENT): Buildup factor in ANS standard obtained by the moment methods[2)]

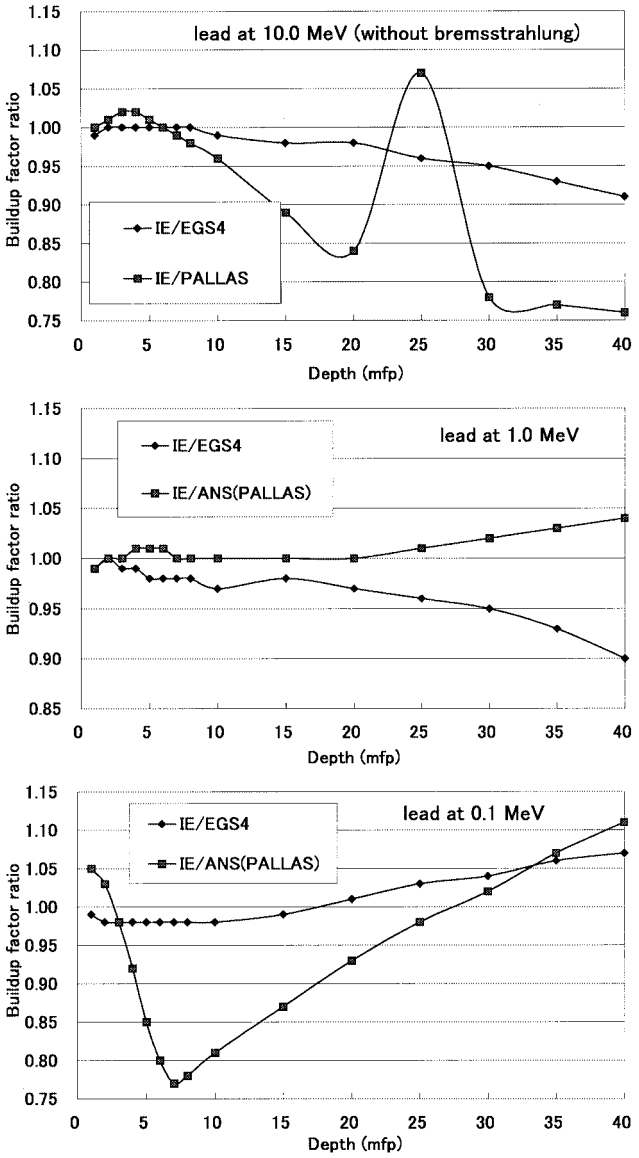

Fig. 6 Ratio of exposure buildup factor for lead obtained by IE method to that obtained by other method
IE: Present calculation
EGS4: Buildup factor obtained by using EGS4[6)]
ANS(PALLAS): Buildup factor in ANS standard obtained by using PALLAS[2)]
PALLAS: Buildup factor obtained by using PALLAS[23)]

40 mfp in our calculations, provided that EGS4 data may have an error of the same magnitude as IE data due to the particle splitting technique.

(3) Comparison with Calculations by PALLAS

IE data agrees very well with ANS data computed by using PALLAS code for lead at the source energy of 1.0 MeV. A discrepancy more than 20%, however, is found between IE data and ANS data obtained by PALLAS for lead at he source energies of 0.1 MeV and data obtained by PALLAS[23)] for lead at the source energy of 10 MeV without bremsstrahlung. Judged from the irregularity observed in the curve of the ratio of IE data to PALLAS data as a function of depth, the discrepancy is presumed due to the approximation used in PALLAS, that neglects within-group scattering and requires very fine space mesh.

V. Conclusion

The method of invariant embedding has been applied to calculations of gamma-ray exposure buildup factors for point isotropic sources in infinite homogeneous media up to depths of 100 mfp. Both the method of direct numerical integration and the angular eigenvalue method are used to get solutions. It is shown that the calculations of buildup factors can easily be extended to large depths by both methods.

A comprehensive survey for exposure buildup factors was performed to estimate errors due to energy, angle and space meshes adopted in the transport calculations by the present method. It is confirmed that the error due to space mesh in the present method is 0.03% or less up to depths of 100 mfp.

A method to determine the limiting value of errors associated with angle and energy meshes is developed and applied. It is confirmed numerically that the exposure buildup factors can be computed up to depths 100 mfp with an error less than 10% by using the present method.

The exposure buildup factors for water, iron and lead at typical source energies of 10 MeV, 1.0 MeV and 0.1 MeV are provided without bremsstrahlung up to depths of 100 mfp. Those buildup factors are found to agree well with other data including the moments method calculations and the Monte Calro calculations by EGS4.

These results indicate that the method of invariant embedding is able to provide gamma-ray exposure buildup factors up to depths of 100 mfp with an accuracy enough to be used in shielding calculations.

References

1) H. Goldstein, J. E. Wilkins, Jr., *Calculations of the Penetration of Gamma Rays*, NYO-3075, (1954).
2) American National Standard, *Gamma-Ray Attenuation Coefficients and Buildup Factors for Engineering Materials*, ANSI/ANS-6.4.3, (1991).
3) K. Takeuchi, S. Tanaka, *PALLAS-1D (VII); A code for direct integration of transport equation in one dimensional plane and spherical geometries*, JAERI-M84-214, (1984).
4) Y. Harima, "Validity of the geometrical progression formula in approximating gamma-ray buildup factor," *Nucl. Sci. Eng.*, **94**, 24 (1986).
5) Y. Harima, "An historical review and current status of buildup factor calculations and applications," *Radiat. Phys. Chem.*, **41**, 631 (1993).
6) H. Hirayama, "Calculation of gamma-ray exposure buildup factors up to 40 mfp using the EGS4 Monte Carlo code with a particle splitting," *J. Nucl. Sci. Technol.*, **32**, 1207 (1995).
7) A. Kitsos, *et al*., "Determination of point isotropic buildup factors of gamma rays including incoherent and coherent scattering for aluminum, iron, lead, and water by the discrete ordinate method," *Nucl. Sci. Eng.*, **117**, 49 (1994).
8) A. Kitsos, *et al*., "Improvement of gamma-ray S_n transport calculations including coherent and incoherent scatterings and secondary sources of bremsstrahlung and fluorescence: Determination of gamma-ray buildup factors," *Nucl. Sci. Eng.*, **123**, 215 (1996).
9) A. Shimizu, "Development of angular eigenvalue method for radiation transport problems in slabs and its application to penetration of gamma rays," *J. Nucl. Sci. Technol.*, **37**, 15 (2000).
10) O. Chibani, "New photon exposure buildup factors," *Nucl. Sci. Eng.*, **137**, 215 (2001).
11) J. H. Hubbell, *Photon Cross Sections, Attenuation Coefficients and Energy Absorption Coefficients from 10 keV to 100 GeV*, NSRDS-NBS29, (1969).
12) Radiation Shielding Information Center Data Package DLC-136/PHOTX, contributed by Natl. Inst. of Standards and Technol.
13) H. Hirayama, D. K. Trubey, "Effects of incoherent and coherent scattering on the exposure buildup factors of low energy gamma rays," *Nucl. Sci. Eng.*, **99**, 145 (1988).
14) V. Ambarzumian, *Compt. Rend Acad. Sci. USSR*, **38**, 299 (1943).
15) S. Chandrasekhar, *Radiative Transfer*, Oxford Univ. Press, (1950).
16) R. Bellman, R. Kalaba, *Proc. Natl. Acad. Sci. USA*, **42**, 629 (1956).
17) A. Shimizu, H. Mizuta, "Application of invariant imbedding to the reflection and transmission problem of gamma rays (I)," *J. Nucl. Sci. Technol.*, **3**, 57 (1966).
18) A. Shimizu, H. Mizuta, "Application of invariant imbedding to the reflection and transmission problem of gamma rays (II)," *J. Nucl. Sci. Technol.*, **3**, 441 (1966).
19) A. Shimizu, "Calculation of the penetration of gamma rays through slabs by the method of invariant embedding," *Nucl. Sci. Eng.*, **32**, 385 (1968).
20) A. Shimizu, K. Aoki, *Application of Invariant Embedding to Reactor Physics*, Academic Press, (1972).
21) H. Kadotani, A. Shimizu, "Gamma ray albedo data generated by the invariant embedding method," *J. Nucl. Sci. Technol.*, **35**, 584 (1998).
22) E. E. Morris, "Moments method calculation of buildup factors for point isotropic monoenergetic gamma-ray sources at depths greater than 20 mean-free-paths," *Nucl. Sci. Eng.*, **99**, 145 (1988).
23) H. Hirayama, *et al*., "A comparison of gamma-ray point isotropic buildup factors including fluorescence and bremsstrahlung in lead using discrete ordinate and point Monte Carlo method," *J. Nucl. Sci. Technol.*, **27**, 524 (1990).